Organic Process Research & Development

Article

pubs.acs.org/OPRD

Optimization of Reductive Debenzylation of Hexabenzylhexaazaisowurtzitane (the Key Step for Synthesis of HNIW) Using Response Surface Methodology

Yadollah Bayat,* Heshmat Ebrahimi, and Farshad Fotouhi-Far

Department of Chemistry and Chemical Engineering, Malek Ashtar University of Technology, P.O. Box 16765-3454, Tehran, Iran

Supporting Information

ABSTRACT: Reductive debenzylation of hexabenzylhexaazaisowurtzitane (HBIW) was carried out using palladium hydroxide deposited on activated carbon catalyst. The catalyst has been characterized using a nitrogen adsorption/desorption isotherm, a hydrogen isotherm, scanning electron microscopy (SEM), and transmission electron microscopy (TEM). The synthesized catalyst showed pore sizes larger than 20 Å, which are attributed to mesopore structures. A multivariate optimization approach was developed by means of central composite design (CCD) for optimizing reaction conditions. The influence of four variables, including the catalyst to HBIW (**1**) relative percent, reaction temperature, hydrogen pressure, and acetic anhydride (Ac_2O), on the reaction yield was investigated. The results showed that the optimum parameters for reductive debenzylation were 20% (w/w) for catalyst to HBIW (**1**) percent, 48.5 °C for reaction temperature, 4.25 bar for hydrogen pressure, and 10.9 for Ac_2O/HBIW mole ratio. Under these conditions, the reaction yield increased to 73%.

1. INTRODUCTION

High energy density materials such as polynitropolyaza-caged compounds are candidate materials for increasing rocket, gun propellant, and explosive performance. Hexanitrohexaazaisowurtzitane (HNIW or CL-20) is one of the most important high energy density materials, which has higher energy and density than those of monocyclic nitramines, such as cyclotetramethylene tetranitramine (HMX) and cyclotrimethylene trinitramine (RDX).[1] Compared to other nitramines, HNIW (**4**) has six N-NO2 groups in its polycyclic structure, resulting in an increase in both density and heat of formation.[2] HNIW-based formulations yield a 42% increase in total energy and a 28% increase in expansion energy over HMX/RDX-based formulations. Due to the high energy content of these cagelike molecules, the detonation pressure is very high: more than double that of TNT.[3] The propellants or explosives composed of HNIW (**4**) are expected to increase the performance in specific impulse, burning rate, ballistic, and detonation velocity.[4]

Nielsen and co-workers proposed and performed a synthesis route for producing HNIW (**4**).[5] Accordingly, all known methods of producing HNIW (**4**) based on the same starting material, 2,4,6,8,10,12-hexabenzyl-2,4,6,8,10,12-hexaazaisowurtzitane (HBIW (**1**)), are first reductively acylated to form 2,6,8,12-tetraacetyl-4,10-dibenzyl-2,4,6,8,10,12-hexaazaisowurtzitane (TADB (**2**)).[5] Then the remaining benzyl groups can be removed either by reductive formylation, with the formation of 2,6,8,12-tetraacetyl-4,10-diformyl-2,4,6,8,10,12-hexaazaisowurtzitane (TADFIW (**3**)),[6] or by nitrosation, leading to 2,6,8,12-tetraacetyl-4,10-dinitroso-2,4,6,8,10,12-hexaazaisowurtzitane (TADNIW).[5,7] Both are easily converted to HNIW (**4**) by nitration with different nitrating systems.[5,7] However, direct nitration of HBIW (**1**) to HNIW (**4**) by nitrolysis is abortive because of the competing nitration of phenyl rings[8] and thereby necessitates debenzylation by catalytic hydrogenation prior to nitration. The synthesis steps of HNIW (**4**) are presented in Scheme 1. The first step, conversion of HBIW (**1**) to TADB (**2**), is the major challenge of the HNIW (**4**) synthesis.

Pd is particularly efficient as a catalyst in hydrogenolysis reactions. In order to gain a great potential, palladium is usually supported on porous materials in the form of extremely small particles.[9] This is because metal catalyst particles can be dispersed to a greater degree and, therefore, are exposed to a larger number of substrate molecules. Activated carbons have

Scheme 1. Schematic Conversion of HBIW to HNIW

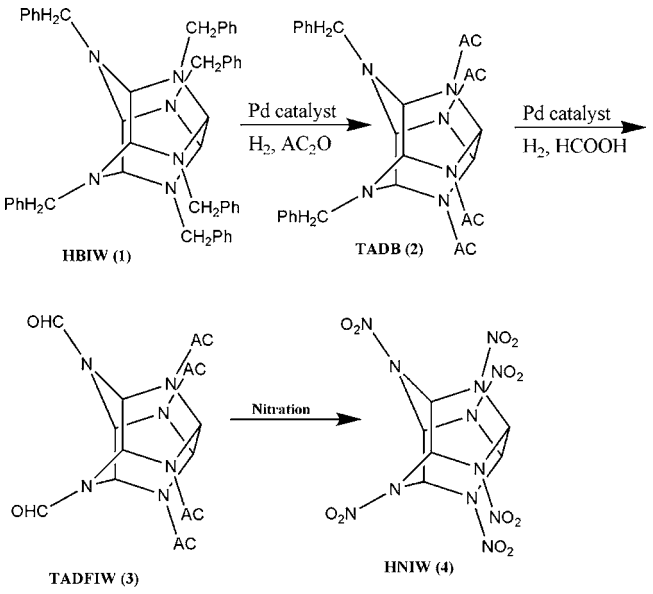

Received: June 18, 2012
Published: October 11, 2012

   dx.doi.org/10.1021/op300162d | *Org. Process Res. Dev.* 2012, 16, 1733−1738

some advantages as catalyst support. They are relatively inexpensive, possess a high surface area, allow easy recovery of supported metal by simple combustion of the support, show chemical inertness both in acidic and basic media, and at the same time do not contain very strongly acidic centers on their surface, which could provoke undesirable side reaction during the catalytic run.[10] Up to 75% of hydrogenolysis reactions are currently carried out over Pd/C catalysts.[11] Most of the investigations for TADB (**2**) production from HBIW (**1**) were carried out by palladium catalyst on activated carbon.[12,13] Some attempts were made to optimize the requirement of the Pd catalyst as an economy measure.[14−16]

Response surface methodology (RSM), a branch of experimental design methodology, introduced by Box and Wilson,[17] is useful for the evaluation of the effects of multiple factors and their interactions and can be effectively used to find the combinations of these factors, which will produce an optimal response. It is advantageous compared with univariate optimization because it allows the achievement of optimum conditions with a few experiments and permits the observation of the interactions between variables, which is not possible when univariate approaches are used. Central composite design (CCD), a second-order technique of RSM, makes it easy to arrange and interpret experiments in comparison with others, and is widely applied in many studies. Over the past decades, some researchers have applied experimental design methodology for controlling different factors affecting heterogeneous catalytic reactions. Cukic et al. applied D-optimal design as a well-known design of experiment (DoE) approach for evaluating the influence of preparation variables on the performance of the Pd/Al_2O_3 catalyst in the hydrogenation of 1,3-butadiene.[18] A fractional factorial design as another DoE approach was applied to investigate the influence of seven preparation factors on the hydrogenolysis of aryl halides by pd/C catalysis.[19] Blondet et al. employed an experimental design methodology to optimize the hydrogenation of nitrotoluene using Pd supported on chitosan hollow fibers.[20]

The aim of the present investigation was to optimize the catalytic conversion of HBIW (**1**) to TADB (**2**) by employing response surface methodology. The effects of palladium catalyst loading, reaction temperature, reaction time, and acetic anhydride (Ac_2O) stoichiometry on the yield of the reaction were systematically analyzed using CCD.

2. EXPERIMENTAL SECTION

2.1. Chemicals and Materials. HBIW (**1**) as a precursor material for HNIW (**4**) was synthesized as proposed in ref 21 and primarily washed with ethanol and then recrystallized from ethyl acetate. Purified HBIW (**1**) was characterized by measuring its melting point and TLC. DMF, acetic anhydride, and bromobenzene were supplied by Merck (Germany) and were used as a cosolvent, acetylation reagent, and cocatalyst, respectively. $PdCl_2$ was purchased locally. Activated carbons and sodium carbonate, which were used as catalyst support and basic agent, were both Merck grade (see Supporting Information). Deionized water was also used throughout the study. Synthesized TADB (**2**) samples were characterized by melting point (315−317 °C) and TLC. These two techniques revealed that the synthesis TADB was pure. In addition, the FT-IR and ^1H NMR spectra of the product completely complied with published data.[22,23]

2.2. Characterization of Catalyst. The nitrogen adsorption/desorption isotherm was measured at 77 K using a Micromeritics ASAP 2010 instrument. Catalyst sample had been degassed under vacuum for 3 h at 150 °C prior to measurement. The specific surface and pore size distribution were calculated using both Brunauer, Emmett, and Teller (BET) and Barrett−Joyner−Halenda (BJH) models, respectively. Chemical adsorption (chemisorption) analyses can provide much of the information needed to evaluate catalyst materials. So, the hydrogen adsorption isotherm was used to measure the active surface of the catalyst and also the distribution of the palladium on the surface of the catalyst. In this regard, catalyst samples were held under vacuum at 400 °C. Then, the temperature was decreased to 30 °C and hydrogen pressure was increased for recording the isotherm.

Scanning electron microscopy (SEM) and transmission electron microscopy (TEM) were utilized to evaluate the surface topology of the catalyst. SEM and TEM images (see Figure 5) were obtained by Hitachi S4160 and Philips S4160 instruments, respectively.

Finally, the loading percent of palladium on the catalyst was measured by inductively coupled plasma (ICP) analysis.

2.3. Reductive Debenzylation of HBIW. The catalytic debenzylation of HBIW (**1**) was carried out in a 2 L stainless steel reactor (Buchi bmd 075) equipped with a turbine stirrer (18.6 rpm), a temperature probe, a heating jacket, and a system of gaseous hydrogen supply. A schematic representation of the experimental setup is shown in Figure 1.

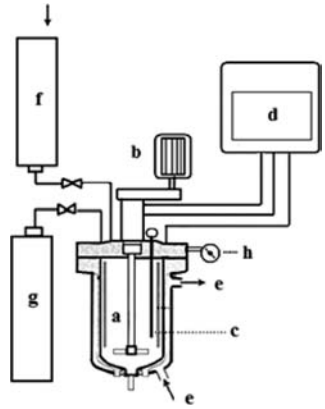

Figure 1. Schematic representation of experimental set up: (a) impeller; (b) motor; (c) thermocouple; (d) temperature and agitation speed control panel; (e) oil circulation; (f) hydrogen cylinder; (g) nitrogen cylinder; (h) pressure gauge.

Each experiment was carried out by mixing HBIW (**1**) (5 g, 7 mmol) in dimethylformamide (DMF; 50 mL, 10 volumes) with freshly synthesized palladium catalyst (0.25−1 g, 5−20 wt %) according to the planned experiments. As suggested by Koskin et al.,[24] bromobenzene (0.45 mL, 4.28 mmol), a source of hydrogen bromide, was added to the reaction mixture as a cocatalyst. The hydrogenolysis of the C−N bond can be accelerated in the presence of PhBr. Thereafter, acetic anhydride (Ac_2O; 5−10 mL, 53−106 mmol) as acetylating agent was added to the mixture. During the reaction, the hydrogen pressure and reaction temperature were kept between the values of 2.5−6 bar and 35−55 °C, respectively. The hydrogenolysis was performed over a 4 h period. At the end of an experiment, catalyst and the product (TADB (**2**)) were filtered off (sinter porosity 4) and were rinsed with acetone. Precipitated TADB was dissolved in acetic acid, and then the

dx.doi.org/10.1021/op300162d | Org. Process Res. Dev. 2012, 16, 1733−1738

catalyst was filtered and methanol was added to the solution of TADB and acetic acid. After a while white crystals of TADB started to precipitate, and after 2 or 3 h, the precipitation process of TADB crystals was completed. The TADB crystals were filtered and dried.

2.4. Data Analysis. A central composite design (CCD) was applied to optimize the effective parameters. This is the most popular class of designs used for fitting second order models. Generally, for F factors, the CCD consists of $N_F = 2^F$ factorial or fractional factorial points with coordinates in coded values as $x_i = +1$ or $x_i = -1$ for the $i = 1, .., F$; $N_\alpha = 2F$ axial or star points with all their coordinates zero except for the one, which is set equal to a certain value ($+\alpha$ or $-\alpha$). The value of α for rotatable designs depends on the number of points in the factorial position ($\alpha = (N_F)^{1/4}$). Finally, N_C center points, where all the factors have zero coordinates, are performed to assess the pure experimental error of the design.

Inspection of previous works[24−26] and our experience showed that, among different parameters affecting the debenzylation reaction, the four parameters, catalyst to HBIW (**1**) percent (A), reaction temperature (B), hydrogen pressure (C), and acetic anhydride amount (D), might have an impact on the reaction yield. Therefore, the effects of these parameters on the yield of the reaction (yield %) were evaluated. The coded and actual values of the factors are shown in Table 1.

Table 1. Factors and Their Levels for Central Composite Design (CCD)

	levels				
variables	−1.68	−1	0	1	1.68
A: Catalyst %	5	8	12.5	17	20
B: Temperature (°C)	35	39	45	51	55
C: Pressure (bar)	2.5	3.21	4.25	5.29	6
D: Ac_2O/HBIW (mol ratio)	7.5	9.1	11.4	13.6	15.1

The sequence of experiments was randomized in order to minimize the effects of uncontrolled parameters. The complete design matrix of the experiments, requiring 21 experiments, is shown in Table 2.

Statistical analysis and response surface graphs were generated using the Design-Expert 7 software (State Ease Inc., Minneapolis, MN, USA).

3. RESULTS AND DISCUSSION

3.1. Characterization of the Catalyst. The nitrogen adsorption/desorption isotherm and pore size distribution of the catalyst are shown in Figures 2 and 3.

A typical condensation was observed above the relative pressure of 0.5, reflecting the presence of mesopores. The calculated specific surface area, volume of nitrogen monolayer, and total pore volume under relative pressure 0.99, respectively, were equal to 147 m^2/g, 23 cm^3/g, and 0.13 cm^3/g.

The hydrogen adsorption isotherm is presented in Figure 4.

It can be seen that hydrogen adsorption increases with pressure to reach a plateau at a pressure of about 4−8 kPa. We could notice that all active sites of the catalyst were saturated at this pressure. Table 3 presents the properties of the catalyst measured by the hydrogen isotherm.

The SEM and TEM images of the catalyst and support are given in Figure 5.

Table 2. Design Matrix and the Responses for Central Composite Design

run	A	B	C	D	yield %
1	8	51	5.29	13.6	7.6
2	8	39	3.21	9.1	25.8
3	12.5	45	4.25	15.1	10.4
4	12.5	45	4.25	11.4	37.2
5	8	51	3.21	13.6	13.5
6	12.5	45	4.25	11.4	34.8
7	12.5	45	4.25	11.4	40.2
8	17	39	3.21	13.6	27.1
9	12.5	55	4.25	11.4	16.2
10	12.5	45	4.25	11.4	35.3
11	12.5	45	4.25	11.4	33.2
12	20	45	4.25	11.4	70.3
13	12.5	45	4.25	7.5	24.6
14	17	51	5.29	9.1	47.9
15	17	39	5.29	13.6	23.5
16	8	39	5.29	9.1	24.4
17	12.5	45	6	11.4	36.6
18	5	45	4.25	11.4	30.0
19	12.5	45	2.5	11.4	37.4
20	17	51	3.21	9.1	46.2
21	12.5	35	4.25	11.4	12.6

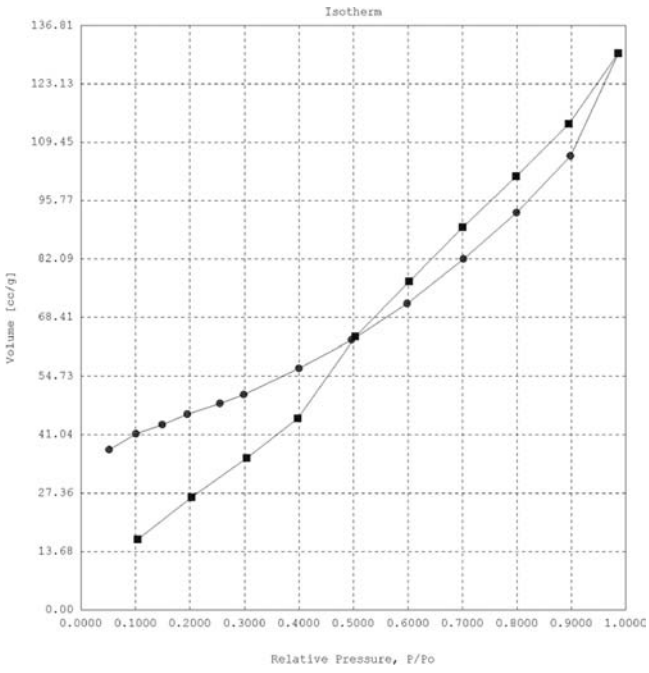

Figure 2. Adsorption/desorption isotherm of nitrogen on $Pd(OH)_2/C$ catalyst at 77 K.

As can be seen, almost all surfaces of activated carbon were covered by $Pd(OH)_2$ clusters. The average size of the $Pd(OH)_2$ particles was about 15 nm. According to the TEM image, palladium particles were uniformly distributed across the surface of activated carbon.

3.2. Response Surface Methodology. There were a total of 21 experiments for optimizing the four individual parameters via a reduced central composite design. A reduced central composite design was used, since experimental runs were expensive and time-consuming. The response values are listed in Table 2. Evaluation of various models through analysis of

dx.doi.org/10.1021/op300162d | Org. Process Res. Dev. 2012, 16, 1733−1738

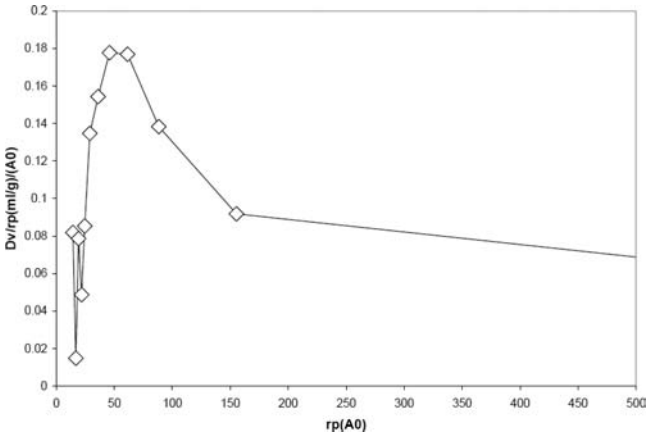

Figure 3. Pore size distribution of $Pd(OH)_2/C$ catalyst.

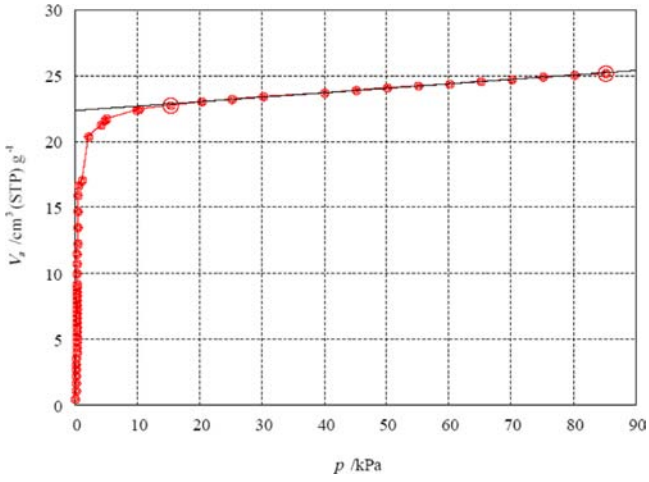

Figure 4. Adsorption isotherm of hydrogen on $Pd(OH)_2/C$ catalyst.

Table 3. Catalyst Properties Based on the Hydrogen Adsorption Isotherm

H.A.[a] (cm^3/g)	A.S.$_{catalyst}$[b] (m^2/g)	A.S.$_{metal}$[c] (m^2/g)	% Pd	% Distr[d]	P.S.$_{ave}$[e] (nm)
11	47	358	13	79	1.5

[a]Hydrogen adsorption. [b]Active metal based on catalyst. [c]Active metal based on whole metal of catalyst. [d]Particles distribution. [e]Average of particle size.

variance (ANOVA) and the statistical parameters revealed that a second-order polynomial model is adequate for describing variation of the response within the experimental domain. The ANOVA table of the model is presented in Table 4.

Analysis of variance partitions the total variation in the data into variation due to the factors (main factors and their interaction terms) and those due to the random factors. These components of variation were then used to calculate an *F*-value. The calculated *F*-values are compared with the tabulated *F* distribution to designate at which probabilities (*p*-value) the factors are significant. A *p*-value less than 0.05 for a model term indicates that it is significant at the 95% probability level. The *p*-value for the lack of a fit test is large ($p = 0.8115$), and so the hypothesis that the tentative model adequately describes the data cannot be rejected, implying that the quadratic model is adequate (more details about the model are presented in the

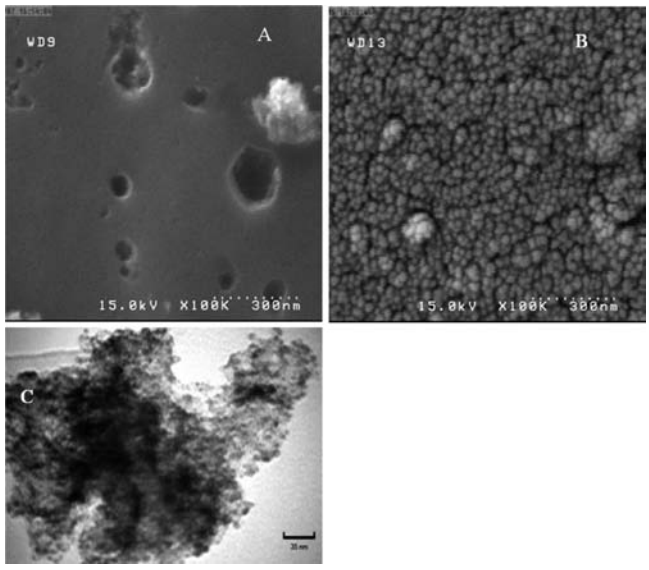

Figure 5. (a) SEM image of bare activated carbon. (b) SEM image of the $Pd(OH)_2/C$ catalyst. (c) TEM image of the $Pd(OH)_2/C$ catalyst.

Supporting Information). Equation 1 expresses the reaction yield as a function of the coded factor levels.

$$\text{yield } \% = 36.41 + 12.02A + 1.49\text{B} - 4.17D + 4.86AB + 2.85BD + 4.89A^2 - 7.73B^2 - 6.59D^2 \quad (1)$$

where *A*, *B*, and *D* are model terms that represent the operating factors of catalyst to HBIW (**1**) percent, reaction temperature, and acetic anhydride amount, respectively. It can be seen that hydrogen pressure shows no significant effect on the reaction within the ranges tested.

The effects of catalyst to HBIW (**1**) percent, reaction temperature, and acetic anhydride, as well as their interactions, are shown in Figure 6.

Catalyst percent was found to be the most significant factor, whereas hydrogen pressure was found not to have a significant effect on the measured response. This figure shows a tendency of response enhancement with increasing catalyst percent. This is not surprising, since increasing catalyst percent presents a much more active site for the substrate and, therefore, enhances the probability of the reaction proceeding. It is seen that increasing the reaction temperature up to 48 °C causes an increase in the reaction efficiency, but further enhancement of the reaction temperature may cause slight damage to HBIW (**1**) or activate other reaction pathways. So, the reaction yield decreases at high values of the reaction temperature. Based on the response surface (Figure 6), acetic anhydride exhibits a dual effect on the reaction yield. Increasing the Ac_2O/HBIW mole ratio from 9.1 to 10.6 enhanced the reaction yield, while with increasing of Ac_2O concentration a gradual decline in reaction yield was observed. This behavior is also observed by Koskin et al.[24] They claimed that excess of the acylating agent accelerates side reactions, and its deficiency leads to a decrease in acylation rate. The main objective of the response surface methodology is to optimize the effective factors affecting the response. In order to optimize the process, values of the factors were considered in the range of ($\pm\alpha$) and the maximum value was obtained for the yield. According to this procedure, the optimum values of the factors were 20% (w/w) for the catalyst to HBIW (**1**) percent, 48.5 °C for the reaction temperature, 2.5−6.0 bar for hydrogen

dx.doi.org/10.1021/op300162d | Org. Process Res. Dev. 2012, 16, 1733−1738

Table 4. Analysis of Variances (ANOVA) Table of the Quadratic Response Surface Model

source	S.S.	d.f.	M.S.	*F*-value	*p*-value	
model	4243.9	8	530.5	108.5	<0.0001	significant
A	817.7	1	817.8	167.2	<0.0001	
B	30.4	1	30.4	6.2	0.0282	
D	98.8	1	98.8	20.2	0.0007	
AB	78.1	1	78.1	15.9	0.0018	
BD	27.0	1	27.0	5.5	0.0367	
A^2	358.3	1	358.3	73.2	<0.0001	
B^2	897.7	1	897.6	183.5	<0.0001	
D^2	659.4	1	659.4	134.8	<0.0001	
residual	58.7	12	4.9			
lack of fit	29.4	8	3.8	0.502	0.811	not significant
pure error	29.3	4	7.3			
corrected total	4302.6	20				

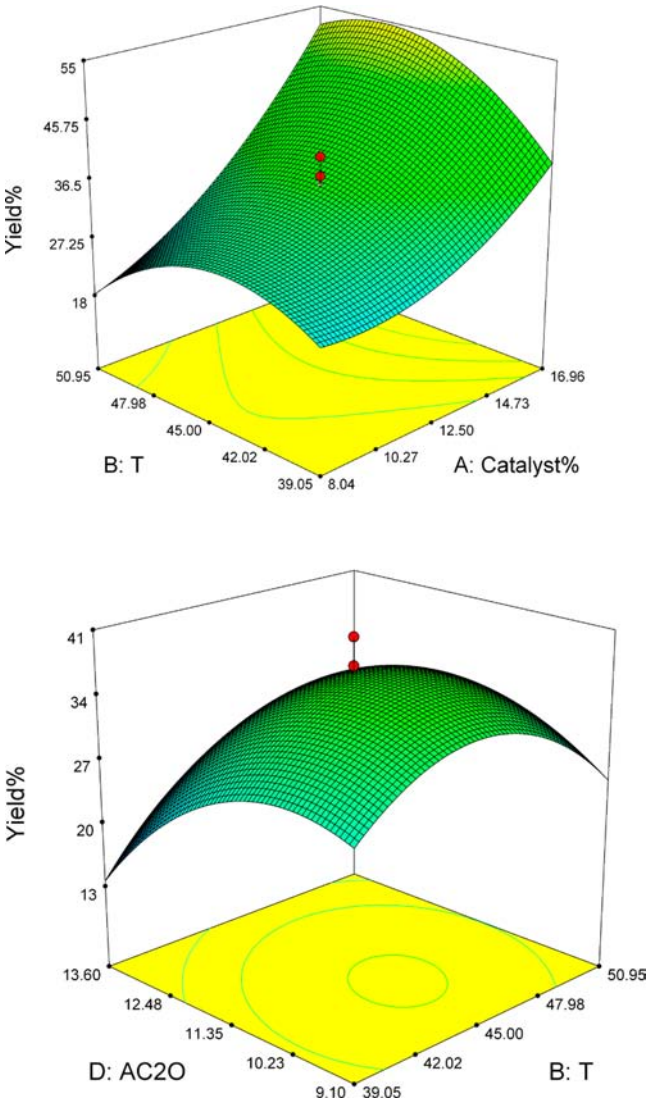

Figure 6. Three-dimensional (3D) response surface for yield as a function of (a, top) catalyst percent (A) and temperature (B) (Ac_2O was set to 11.4); (b, bottom) temperature (B) Ac_2O/HBIW (D) (catalyst percent was set to 12.5).

pressure, and 10.9 for Ac_2O/HBIW ratio. The predicted and experimental values of the reaction yield obtained at the optimum conditions were 75% and 73%, respectively.

4. CONCLUSION

In this study, reductive debenzylation of HBIW (**1**) has been optimized using a central composite design. This design was very efficient for the establishment of the optimum condition. The results demonstrated that the catalyst to HBIW (**1**) relative percent was the parameter shown to have the most pronounce effect on the yield of the reaction. Hydrogen pressure did not have a marked effect on the reaction. Reaction temperature and Ac_2O/HBIW ratio represent a surface curvature shape with a maximum within the domain of the design.

The nitrogen adsorption/desorption isotherm confirms the presence of mesopore structures for the catalyst. According to the hydrogen isotherm, most of the active sites of the catalyst were covered at the hydrogen pressure of about 4−8 kPa. TEM and SEM images confirmed formation of $Pd(OH)_2$ on the surface of the activated carbon.

■ ASSOCIATED CONTENT

Supporting Information

Details of preparation of the catalyst and of the response surface methodology as well as plots of the values of the reaction yield and of the residuals. This material is available free of charge via the Internet at http://pubs.acs.org.

■ AUTHOR INFORMATION

Corresponding Author

*E-mail address: Y_bayat@mut.ac.ir. Telephone: +98-(0)21-22949213.

Notes

The authors declare no competing financial interest.

■ REFERENCES

(1) Bazaki, H.; Kawabe, S.; Miya, H.; Kodama, T. Synthesis and sensitivity of hexanitrohexaaza-isowurtzitane (HNIW). *Propellants, Explos., Pyrotech.* **1998**, *23*, 333−336.

(2) Turcotte, R.; Vachon, M.; Kwok, Q. S. M.; Wang, R.; Jones, D. E. G. Thermal study of HNIW (CL-20). *Thermochim. Acta* **2005**, *433*, 105−115.

(3) Bircher, S. R.; Mader, P.; Mathieu, J. Properties of CL-20 based high explosives. *Annual ICT Conference on Energetic Materials*; Karlsruhe, Germany, 1998.

(4) Chung, K.-H.; Kil, H.-S.; Choi, I.-Y.; Chu, C.-K.; Lee, I.-M. New precursors for hexanitrohexaazaisowurtzitane (HNIW, CL-20). *J. Heterocycl. Chem.* **2000**, *37*, 1647−1649.

(5) Nielsen, A. T.; Chafin, A. P.; Christian, S. L.; Moore, D. W.; Nadler, M. P.; Nissan, R. A.; Vanderah, D. J.; Gilardi, R. D.; George, C.

F.; Anderson, J. L. F. Synthesis of polyazapolycyclic caged polynitramines. *Tetrahedron* **1998**, *54*, 11793−11812.
(6) Agrawal, J. P.; Hodgson, R. D. *Organic Chemistry of Explosives*; John Wiley & Sons: Chichester, U.K., 2007.
(7) Braithwaite, P. C. R.; Hatch, L.; Lee, K.; Wardle, R. B.; Mezger, M.; Nicolich, S. Energetic materials production, processing and characterization. *Annual ICT Conference on Energetic Materials*; Karlsruhe, Germany, 1998.
(8) Nielsen, A. T. Caged polynitramine compound. U.S. patent, 5693794 A, 1997; pp 532−570.
(9) Ohno, M.; Okamura, N.; Kose, T.; Asada, T.; Kawata, K. Effect of palladium loaded activated carbons on hydrogen storage. *J. Porous Mater.* **2012**, *19*, DOI: 10.1007/s10934-012-9567-0.
(10) Gurrath, M.; Kuretzky, T.; Boehm, H. P.; Okhlopkova, L. B.; Lisitsyn, A. S.; Likholobov, V. A. Palladium catalysts on activated carbon supports: Influence of reduction temperature, origin of the support and pretreatments of the carbon surface. *Carbon* **2000**, *38*, 1241−1255.
(11) Osthuizen, R. S.; Nyamori, V. O. Carbon nanotubes as supports for palladium and bimetallic catalysts for use in hydrogenation reactions. *Platinum Metals Rev.* **2011**, *55*, 154−169.
(12) Bellamy, A. J. Reductive debenzylation of hexabenzylhexaazaisowurtzitane. *Tetrahedron* **1995**, *51*, 4711−4722.
(13) Tamotsu, K. Preparation of hexakis (trimethylsilylethylcarbamyl) hexaazaisowurtzitane. Japanese patent, 06321962 A2, 1994.
(14) Wardle, R. B.; Hinshaw, J. C. Multi step synthesis of polycyclic polyamides as precursors for polycyclic polynitramine oxidizers in propellants and explosives. Brit. U.K. Patent, GB 2333292, 1999.
(15) Wardle, R. B.; Hinshaw, J. C. Synthesis and reactions of hexaazaisowurtzitane type compounds in synthesis of hexanitro hexaaza isowurtzitane (HNIW) explosive. U.S. Patent, 6147209 A, 2000.
(16) Ou, Y.; Xu, Y.; Chen, B. Synthesis of hexanitrohexaazaisowurtzitane from tetraacetyldiformylhexazaisowurtzitane. *Chin. J. Org. Chem.* **2000**, *20*, 556−559.
(17) Box, G. E. P.; Wilson, K. B. On the experimental attainment of optimal conditions. *J. R. Stat. Soc.* **1951**, *13*, 1−45.
(18) Cukic, T.; Kraehnert, R.; Holena, M.; Herein, D.; Linke, D.; Dingerdissen, U. The influence of preparation variables on the performance of Pd/Al_2O_3 catalyst in the hydrogenation of 1,3-butadiene: Building a basis for reproducible catalyst synthesis. *Appl. Catal. A: Gen.* **2007**, *323*, 25−37.
(19) Card, R. J.; Schmitt, J. L.; Simpson, J. M. Palladium-carbon hydrogenolysis catalysts: The effect of preparation variables on catalytic activity. *J. Catal.* **1983**, *79*, 13−20.
(20) Blondet, F. P.; Vincent, T.; Guibal, E. Hydrogenation of nitrotoluene using palladium supported on chitosan hollow fiber: Catalyst characterization and influence of operative parameters studied by experimental design methodology. *Int. J. Biol. Macromol.* **2008**, *43*, 69−78.
(21) Nielsen, A. T.; Nissan, R. A.; Vanderah, D. J.; Coon, C. L.; Gilardi, R. D.; George, C. F.; Flippen-Anderson, J. Polyazapolycyclics by condensation of aldehydes with amines. 2. Formation of 2,4,6,8,10,12-hexabenzyl-2,4,6,8,10,12-hexaazatetracyclo-[5.5.0.05.9.03,11]dodecanes from glyoxal and benzylamines. *J. Org. Chem.* **1990**, *55*, 1459−1466.
(22) Talawar, M. B.; Sivabalan, R.; Polke, B. G.; Nair, U. R.; Gore, G. M.; Asthana, S. N. Establishment of process technology for the manufacture of dinitrogen pentoxide and its utility for the synthesis of most powerful explosive of today—CL-20. *J. Hazard. Mater.* **2005**, *124*, 153−164.
(23) Ou, Y.; Jia, H.; Xu, Y.; Chen, B.; Fan, G. Synthesis and crystal structure of β-hexanitrohexaazaisowurtzitane. *Sci. China, Ser. B: Chem.* **1999**, *42*, 217−224.
(24) Koskin, A. P.; Simakova, I. L.; Parmon, V. N. Reductive debenzylation of hexabenzylhexaazaisowurtzitane—the key step of the synthesis of polycyclic nitramine hexanitrohexaazaisowurtzitane. *Russ. Chem. Bull. Int. Ed.* **2007**, *56*, 2370−2375.
(25) Nair, U. R.; Sivabalan, R.; Gore, G. M.; Geetha, M.; Asthana, S. N.; Singh, H. Hexanitrohexaazaisowurtzitane (CL-20) and CL-20-based formulations (review). *Combust. Explos. Shock Waves* **2005**, *41*, 121−132.
(26) Mandal, A. K.; Pant, C. S.; Kasar, S. M.; Soman, T. Process Optimization for Synthesis of CL-20. *J. Energ. Mater.* **2009**, *27*, 231−246.